OXFORD

Human Molecular Genetics, 2016, Vol. 25, No. 2 404–417

doi: 10.1093/hmg/ddv474
Advance Access Publication Date: 24 November 2015
Bioinformatics Article

BIOINFORMATICS ARTICLE

Rheumatoid arthritis-associated RBPJ polymorphism alters memory CD4$^+$ T cells

William Orent[1,†], Allison R. Mchenry[1,†], Deepak A. Rao[2], Charles White[1,3], Hans-Ulrich Klein[1,3], Ribal Bassil[1], Gyan Srivastava[1,3], Joseph M. Replogle[1,3], Towfique Raj[1,3], Michael Frangieh[1], Maria Cimpean[1,3], Nicole Cuerdon[1,3], Lori Chibnik[1,3], Samia J. Khoury[1,4], Elizabeth W. Karlson[2], Michael B. Brenner[2], Philip De Jager[1,3], Elizabeth M. Bradshaw[1,3,*] and Wassim Elyaman[1,3,*]

[1]Ann Romney Center for Neurologic Diseases, [2]Division of Rheumatology, Immunology and Allergy and [3]Program in Translational NeuroPsychiatric Genomics, Department of Neurology, Brigham and Women's Hospital and Harvard Medical School, Broad Institute at Harvard University and MIT, NRB-641, 77 Avenue Louis Pasteur, Boston, MA 02115, USA and [4]Abu Haidar Neuroscience Institute, American University of Beirut Medical Center, Beirut, Lebanon

*To whom correspondence should be addressed. Tel: +1 6175255183; Fax: +1 6175255501; Email: welyaman@rics.bwh.harvard.edu (W.E.); Tel: +1 6175255704; Fax: +1 6175255501; Email: ebradshaw@rics.bwh.harvard.edu (E.M.B.)

Abstract

Notch signaling has recently emerged as an important regulator of immune responses in autoimmune diseases. The recombination signal-binding protein for immunoglobulin kappa J region (RBPJ) is a transcriptional repressor, but converts into a transcriptional activator upon activation of the canonical Notch pathway. Genome-wide association studies of rheumatoid arthritis (RA) identified a susceptibility locus, rs874040^{CC}, which implicated the *RBPJ* gene. Here, chromatin state mapping generated using the chromHMM algorithm reveals strong enhancer regions containing DNase I hypersensitive sites overlapping the rs874040 linkage disequilibrium block in human memory, but not in naïve CD4$^+$ T cells. The rs874040 overlapping this chromatin state was associated with increased RBPJ expression in stimulated memory CD4$^+$ T cells from healthy subjects homozygous for the risk allele (CC) compared with memory CD4$^+$ T cells bearing the protective allele (GG). Transcriptomic analysis of rs874040^{CC} memory T cells showed a repression of canonical Notch target genes IL (interleukin)-9, IL-17 and interferon (IFN)γ in the basal state. Interestingly, activation of the Notch pathway using soluble Notch ligand, Jagged2-Fc, induced IL-9 and IL-17A while delta-like 4Fc, another Notch ligand, induced higher IFNγ expression in the rs874040^{CC} memory CD4$^+$ T cells compared with their rs874040^{GG} counterparts. In RA, RBPJ expression is elevated in memory T cells from RA patients compared with control subjects, and this was associated with induced inflammatory cytokines IL-9, IL-17A and IFNγ in response to Notch ligation *in vitro*. These findings demonstrate that the rs874040^{CC} allele skews memory T cells toward a pro-inflammatory phenotype involving Notch signaling, thus increasing the susceptibility to develop RA.

[†]The first two authors contributed equally to this work.

Received: May 27, 2015. **Revised:** November 3, 2015. **Accepted:** November 15, 2015

Introduction

There is a clear genetic basis to rheumatoid arthritis (RA). To date, ~100 risk loci have been identified, which explain ~20% of variance in disease risk (1–8). Genome-wide association studies of RA identified a susceptibility locus, rs874040^{CC}, which implicated the recombination signal-binding protein for immunoglobulin kappa J region (*RBPJ*) gene. Although the cause of RA is unknown, autoimmunity plays a pivotal role in its pathogenesis. CD4$^+$ T cells recruited into the RA synovium have been thought to drive the synovial inflammation by stimulating the production of pro-inflammatory cytokines from macrophages, synovial fibroblasts and other infiltrating leukocytes (9). The majority of CD4$^+$ T cells in RA synovium belong to the memory CD4$^+$ pool, which correlates with the chronicity and progression of the disease (10,11). Autoimmune diseases such as RA arise from inappropriate immune responses against self-antigens and involve both adaptive and innate immune cells. Targeting of cytokines and their associated inflammatory mediators are now established as a feasible method for treating RA, which may occur due to the imbalance of pro- and anti-inflammatory mediators thus leading to the development of chronic synovial inflammation and joint destruction (12). Inflammatory cytokines, that include tumor necrosis factor (TNF)-α, interleukin (IL)-1β, IL-6, IL-17 and the downstream inflammatory mediators produced by activated cells in the arthritic joints are an essential component of the milieu that drives cartilage and bone destruction.

The role of Notch signaling in the regulation of murine and human T helper (Th) cell development is well established (13,14). The canonical Notch signaling cascade is initiated when a Notch receptor engages a Notch ligand expressed on a neighboring cell. In humans, the classic Notch signaling pathway consists of four heterodimeric trans-membrane receptors (Notch 1–4) and their ligands (Delta-like 1, 3 and 4 and Jagged 1 and 2). The Notch receptor engagement by its ligand triggers a series of enzymatic reactions leading to the release of the Notch receptor intracellular domain that translocates to the nucleus and forms an active transcription complex with the RBPJ region and the co-activator mastermind-like proteins, thus converting RBPJ from a transcriptional repressor to a transcriptional activator (14). During the past few years, the Notch pathway has emerged as an important regulator of effector and regulatory T-cell differentiation and activation (15,16). Notch can induce IL-4 expression by physically interacting with GATA3 (17,18), but can also directly activate the transcription of *Tbx21* to promote Th1-cell differentiation (19) and RORγt to induce the development of murine and human Th17 cells (20). Recently, we demonstrated that Delta-like 4 (DLL4), a Notch ligand, inhibits Treg development by suppressing STAT5 activation thus promoting autoimmune responses in a mouse model of multiple sclerosis (15). In another study, we showed that Notch stimulation converted memory CD4$^+$ T cells into IL-9-producers, which is mediated by Notch/RBPJ complex binding to the *Il9* promoter (21). Inhibition of Notch signaling either pharmacologically, genetically or using biologics that block Notch ligands or receptors, has been shown to be effective in ameliorating the clinical disease in animal models of human diseases including RA (22), multiple sclerosis (21,23) and type 1 diabetes (24). These findings suggest that Notch pathway may be a promising target for RA therapy.

Here, we analyzed the influence of an RA susceptibility locus, rs874040^{CC} in the *RBPJ* region (7) on the adaptive immune system. Of note, rs874040 is in high linkage disequilibrium (LD) with the type 1 diabetes single-nucleotide polymorphism (SNP) rs10517086, thus this association may be shared by the two diseases (25). The rs874040 overlaps a transcriptional enhancer in memory CD4$^+$ T cells, but not in naïve CD4$^+$ T cells. To understand the functional relevance of this polymorphism, we leveraged a cohort of genotyped healthy subjects. We found that memory T cells bearing the rs874040^{CC} risk allele exhibit increased *RBPJ* expression and an alteration of their cytokine profile compared with memory T cells carrying the protective allele. We also found increased *RBPJ* expression in RA patients compared with healthy controls. Our data suggest that RA susceptibility is mediated, in part, by the activation of Notch signaling in memory T cells.

Results

Rs874040 lies over a putative enhancer upstream of RBPJ in memory CD4$^+$ T cells

Chromatin-state annotation using combinations of chromatin modification patterns provides a systematic means for the detection of *cis*-regulatory elements, given the central role of chromatin in mediating regulatory signals and controlling DNA access, and the paucity of recognizable sequence signals. In order to understand whether rs874040 allele status can impact gene regulation, we utilized chromatin states annotation of the human reference genome predicted using the chromHMM algorithm (26) with 15-state model parameters that are provided by the NIH Roadmap Epigenomics Consortium in public domain (27). This project have released list of 127 epigenomes including 111 by the Roadmap Epigenomics program (E001–E113) and 16 by ENCODE (E114–E129) spanning diverse cell and tissue types. Here, we used 'E039' and 'E040' tracks reference epigenome from 'Blood & T-cell' subgroup. 'E039' chromatin-state annotation is relevant for primary Th naive cells from peripheral blood (CD4$^+$_CD25$^-$_CD45RA$^+$_Naive_Primary_Cells) whereas 'E040' chromHMM annotation is relevant for primary Th memory cells from peripheral blood (CD4$^+$_CD25$^-$_CD45RO$^+$_Memory_Primary_Cells). The 15-state mnemonics used by chromHMM are available through the consortium web portal. We generated a SNAP plot with chromatin state mapping within a 1 MB region around the reference SNP, rs874040 (500 KB upstream and downstream). We generated memory and naïve CD4$^+$ T cell-specific chromatin state maps using the publicly available ENCODE ChIP-seq data (28) for well-characterized histone modifications to train and annotate the model. Figure 1 shows all the SNPs on chromosome 4 from dbGAP137 (7) within a 1 MB range and their *P*-value of association to RA as recently reported (7). The recombination rate as well as LD were calculated from the Broad SNAP online server (24) and genomic annotation for the hg19 version. Our analysis reveals (i) enhancer regions containing DNase I hypersensitive sites, and (ii) weak transcription marks within the rs874040 LD block and upstream of the *RBPJ* transcription start site (TSS) in memory but not in naïve T cells (Fig. 1A and B). To gain further insights into the association between the SNPs and the enhancer regions, we mapped the LD block in a 100 kb window in naïve and memory T cells. Among 82 SNPs present in this LD block, we identified 8 SNPs in high LD with the reference SNP rs874040 (0.89–0.99). These SNPs are: rs10517086, rs17630466, rs7441808, rs932036, rs6448432, rs12506688, rs11933540 and rs6825116 (Fig. 1B and Supplementary Material, Table S1). We found that rs932036 overlaps with the enhancer boundaries in memory CD4$^+$ T cells (position 26 090 862 on chromosome 4) (Supplementary Material, Table S1). Next, in attempt to understand the influence of the SNP position, within the enhancer region in memory CD4$^+$ T cells, we used position weight matrices from the JASPAR database (117 human TF motifs) and searched

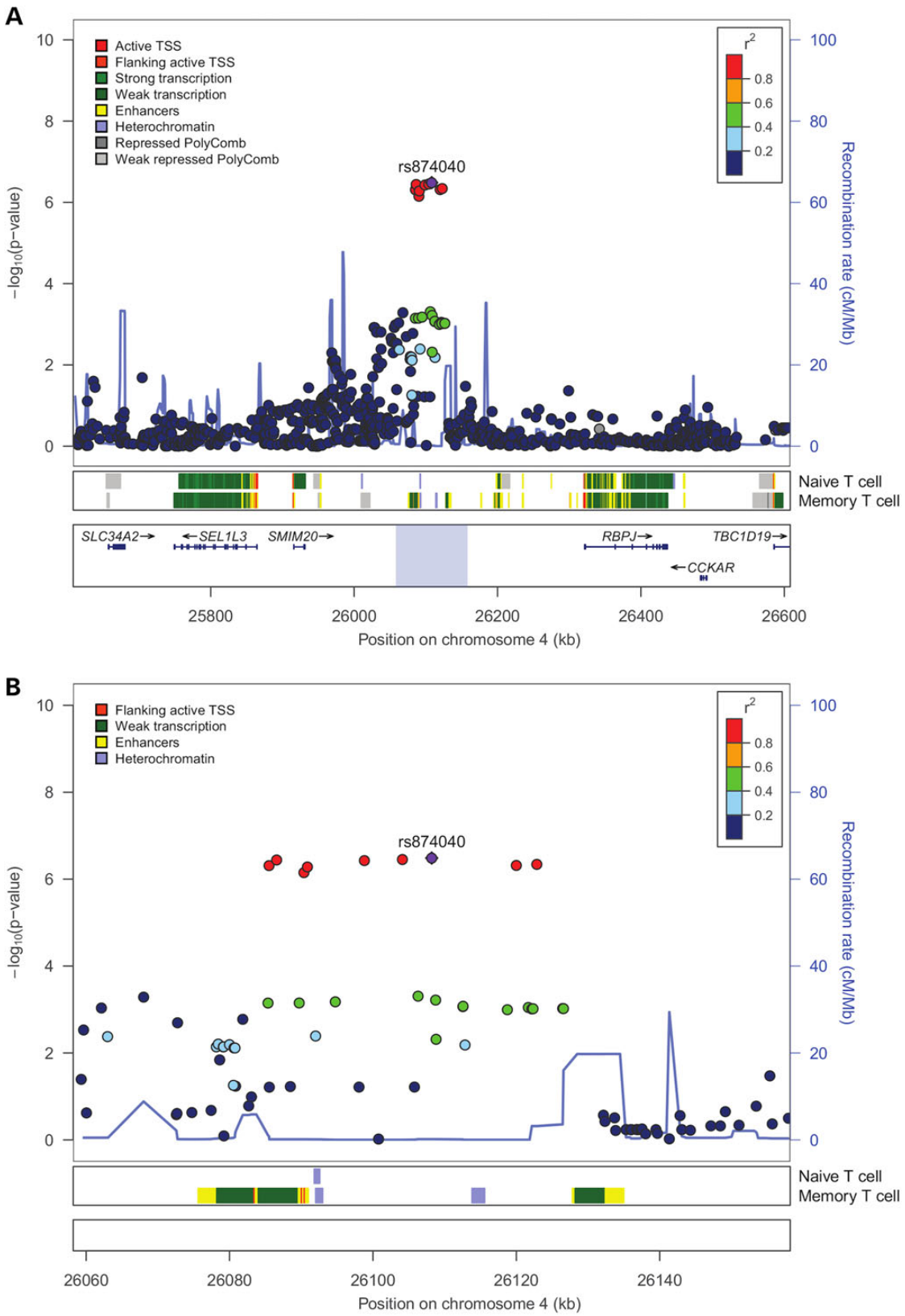

Figure 1. SNAP plots of chromatin state around the rs874040 reveal enhancers and active transcription histone marks in memory CD4$^+$ T Cells. (**A**) Tissue-specific chromatin state mapping were generated using the chromHMM algorithm for naïve CD4$^+$CD25$^-$CD45RA$^+$ and memory CD4$^+$CD25$^-$CD45RO$^+$ T cells as shown in XX and YY. ENCODE ChIP-seq data for various chromatin marks including DNase I hypersensitive sites (enhancers; red), H3K9me3 (heterochromatin; purple), H3K27me3 (polycomb; gray), H3K9ac, H3K4me3 and H3K36me3 (transcription; green) and quiescent regions (other; white) are color-coded. TSS of the three neighboring genes RBPJ, C4orf52 and SEL1L3 are shown (blue). The figure shows all the discovered SNPs from dbGAP137, their *P*-value of association to RA, the recombination rate as calculated from Broad SNAP online server and genomic information for hg19 version at the bottom of the figure. The LD structure is represented in *r*-square value calculated from the Broad SNAP server and is assigned in red color. (**B**) A SNAP plot showing a 100 kb window around the reference SNP rs874040 in both naïve and memory T cells.

for putative binding sites that overlap these SNPs. We show the relative matching score (1 = perfect match) for all TFs and SNPs if the score was ≥0.8 (Supplementary Material, Table S2). We identified potential TF candidates where their binding could be affected by the presence of overlapping SNPs. For instance, the transcription factor ELK1 (ETS domain-containing protein) that is an early response transcription activator and is involved in the induction of the early growth response signaling in T cells (29–31), overlaps the rs932036 (relative matching score = 0.8) (Supplementary Material, Table S2). These findings suggest that the rs932036 risk variant may be involved in the differential *RBPJ* transcription in memory versus naïve CD4$^+$ T cells.

Increased RBPJ expression in rs874040^{CC} memory T cells

To study whether the susceptibility variant rs874040^{CC} regulates *RBPJ* expression, we examined the correlation of the rs874040^{CC} risk allele with changes in the immune profile of healthy subjects. We utilized blood of healthy subjects in order to avoid any confounding effect of immunotherapies or systemic inflammation in patients with autoimmune diseases. We selected healthy genotyped subjects free of autoimmune and chronic infectious diseases who were homozygous for rs874040^{CC} and rs874040^{GG} from the PhenoGenetic Project. We first leveraged the ImmVar data set to examine the effects of the rs874040^{CC} risk allele on *RBPJ* mRNA expression in un-stimulated naïve CD4$^+$CD62L$^+$ T cells isolated from peripheral blood mononuclear cells (PBMCs) of healthy European-American subjects with the susceptibility rs874040^{CC} or the protective rs874040^{GG} allele (n = 213). Expression quantitative trait loci (eQTL) analysis shows that rs874040^{CC} is not correlated with changes in *RBPJ* gene expression in un-stimulated (Fig. 2A) and T-cell receptor (TCR)-stimulated naïve CD4$^+$ T cells (Fig. 2B). Similarly, we did not detect any significant change in the expression of the genes neighboring the rs874040 in naïve T cells (Table 1) or in un-stimulated memory CD4$^+$ T cells as measured by quantitative Taqman PCR (polymerase chain reaction) (Table 2).

Next, we analyzed the gene expression pattern of *RBPJ* in TCR-stimulated naïve CD4$^+$CD45RO$^-$ and memory CD4$^+$CD45RO$^+$ T cells separated from PBMCs of genotyped healthy donors by cell flow sorting. Cells were activated with anti-CD3/CD28 mAb (1 µg/ml), and the mRNA (3 h) and protein (24 h) expression of total RBPJ was assessed by Taqman PCR and enzyme-linked immunosorbent assay (ELISA), respectively. Time points were selected based on the time-course analysis of maximum *RBPJ* mRNA and protein expression upon stimulation (data not shown).

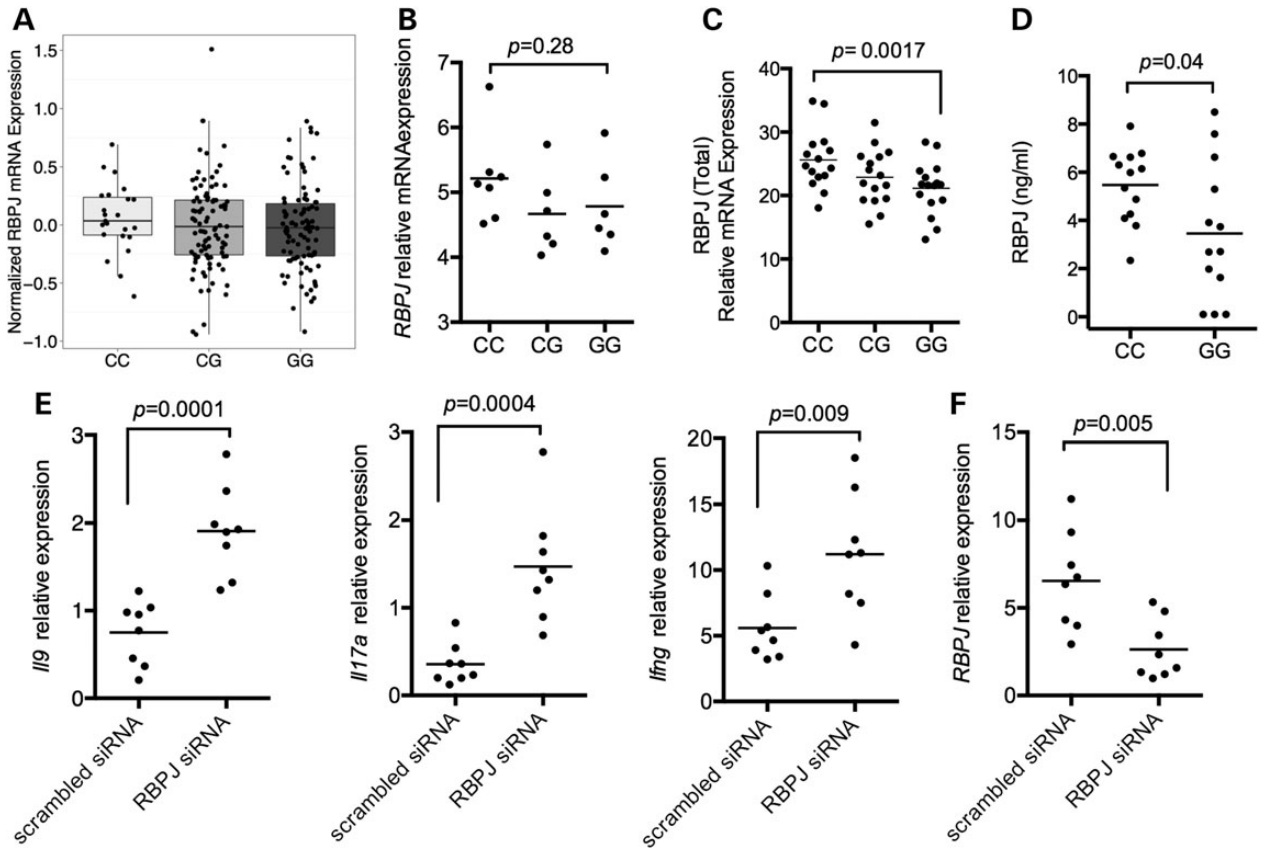

Figure 2. The risk allele rs874040^{C} is associated with increased RBPJ expression in stimulated memory CD4$^+$CD45RO$^+$ T cells from healthy genotyped subjects. (**A**) RBPJ gene expression in naïve CD4$^+$ T cells from 213 healthy European-American subjects, (ρ = 0.016, P = 0.8). The expression data have been adjusted for confounding factors in the model (batch, age and gender). (**B**) Naïve CD4$^+$ T cells were isolated from peripheral blood of healthy subjects bearing risk (CC), protective (GG) or heterozygous for the reference rs874040 allele, cells were stimulated with anti-CD3/CD28 for 3 h and RBPJ expression was measured by Taqman PCR. (**C** and **D**) Memory CD4$^+$CD45RO$^+$ T cells were isolated from peripheral blood of genotyped healthy subjects, cells were stimulated with anti-CD3/CD28 for 3 h and total RBPJ expression measured at the gene level by (C) Taqman PCR and at the protein level by (D) ELISA. Groups were compared by the Wilcoxon matched pairs test and adjusted for batch, age and gender. Each dot represents an individual (n = 12–15/group). (**E** and **F**) RBPJ gene silencing in CD4$^+$ T cells up-regulates inflammatory cytokine expression. Naïve CD4$^+$ cells from healthy donors were transfected with RBPJ siRNA or mock scrambled siRNA by electroporation and cells were incubated in the transfection medium for 4 h. Cells were then harvested, washed and incubated in serum-free medium (X-vivo) with anti-CD3/CD28 for 24 h. (E) Cytokine expression was analyzed by Taqman qPCR normalized to β2-microglobulin. (F) RBPJ mRNA expression in CD4$^+$ T cells transfected with RBPJ siRNA and scrambled siRNA. Data were compared using the unpaired Student t-test.

Table 1. The rs874040 polymorphism does not influence neighboring genes in naïve CD4$^+$ T cells

SNP	Gene	ρ	P-values
rs874040	PI4K2B	−0.067	0.333411778
rs874040	ZCCHC4	−0.05	0.465258637
rs874040	ANAPC4	0.056	0.416016757
rs874040	SLC34A2	−0.024	0.724678665
rs874040	SMIM20	0.043	0.53726912
rs874040	RBPJ	−0.016	0.816305416
rs874040	TBC1D19	0.11	0.110579896
rs874040	STIM2	0.053	0.437365928
rs874040	SEPSECS	0.066	0.339289978
rs874040	SEL1L3	−0.042	0.544067516
rs874040	CCKAR	0.053	0.44554999

The rs874040 *cis*-eQTLs in CD4$^+$CD62L$^+$ T cells of European-American, East Asian and African-American subjects within 1 MB of TSS of a gene and Spearman rank P-values are reported.

Table 2. The rs874040 polymorphism does not influence neighboring genes in un-stimulated memory CD4$^+$ T cells

SNP	Gene	ρ	P-values
rs874040	RBPJ	0.218	0.604
rs874040	SMIM20	0.436	0.28
rs874040	CCKAR	–	–
rs874040	TBC1D19	−0.218	0.604
rs874040	SEL1L3	0	1
rs874040	SLC34A2	–	–

PBMCs were isolated from healthy genotyped subjects ($n = 4$/genotype) and gene expression of six genes neighboring the rs874040 SNP was assessed in memory CD4$^+$CD45RO$^+$ T cells of European-American subjects by quantitative Taqman PCR. Spearman rank P-values are reported. The expression of CCKAR and SLC34A2 in stimulated memory CD4$^+$ T cells was not detected.

We found that healthy donors homozygous for the rs874040^{CC} risk allele have increased *RBPJ* mRNA expression ($P = 0.0017$) in CD4$^+$CD45RO$^+$ memory T cells (Fig. 2C). This was confirmed at the protein level by ELISA, showing significant elevated *RBPJ* expression in CD4$^+$CD45RO$^+$ memory T cells ($P = 0.04$) (Fig. 2D).

Several transcript variants encoding different isoforms have been found for *RBPJ*. To date, four human *RBPJ* isoforms have been described, varying in their N-terminal domain (Supplementary Material, Fig. S1A). Bioinformatic examination of the characterized *RBPJ* transcripts showed that the splice variants contain open reading frames, suggesting that they may generate proteins with similar function. All *RBPJ* transcripts contain a putative nuclear localization signal, an important component of *RBPJ* nuclear translocation to activate target gene transcription (32). Therefore, we carried out an isoform specific quantitative PCR (qPCR) assay in TCR-stimulated memory T cells. We found a rapid increase in Isoform 2 (NM_015874) ($P = 0.042$), Isoform 3 (NM_202283) ($P = 0.0083$) and Isoform 4 (NM_202284) ($P = 8.29 \times 10^{-09}$) 3 h after stimulation of memory T cells from subjects with the rs874040^{CC} risk allele, while the expression of Isoform 1 (NM_005349) was unchanged (Supplementary Material, Fig. S1B).

To determine if the rs874040 risk allele has a specific gene target, we examined gene expression of nearby genes in CD4$^+$ CD45RO$^+$ memory T cells, including SMIM20 and SEL1L3. We did not detect any significant differences in SMIM20 and SEL1L3 expression in TCR-stimulated naïve or memory CD4$^+$ T cells (data not shown).

To validate the repressor function of RBPJ in CD4$^+$ T cells, we utilized an RNA interference approach to knockdown *RBPJ* in T cells. CD4$^+$ T cells isolated from healthy donors were transfected with siRNA specific for human *RBPJ* gene or scrambled siRNA by electroporation, followed by cell activation using anti-CD3/CD28 in serum-free T cell-specific culture medium for 24 h. The cells were then processed for gene expression analysis by Taqman PCR. We found that silencing *RBPJ* in CD4$^+$ T cells up-regulates *Il9*, *Il17a* and *Ifng* expression, which is in agreement with the reported repressive function of RBPJ in T cells (Fig. 2E). Knockdown efficiency was confirmed by measuring *RBPJ* expression in transfected cells (Fig. 2F). To account for multiple comparisons, a Bonferroni-corrected P-value of <0.05/3 was used as the threshold for determining whether siRNA-RBPJ-mediated changes in cytokine expression remained significant. Our analysis shows that RBPJ knockdown regulates significantly *Il9*, *Il17a* and *Ifng* expression (Fig. 2E).

Increased RBPJ expression is associated with repressed canonical Notch target genes in rs874040^{CC} memory T cells

In the absence of canonical Notch signaling, RBPJ acts as a transcriptional repressor. To analyze the influence of rs874040^{CC}-mediated increases in RBPJ expression on memory T-cell phenotype, we sought to measure gene expression of RBPJ-target cytokines particularly interferon (IFN)γ, IL-9 and IL-17A (signature genes of Th1, Th9 and Th17 cells, respectively) and, in addition to other associated genes involved in the abovementioned cell types. To this end, memory CD4$^+$ T cells were isolated by magnetic beads from PBMCs of 46 healthy genotyped subjects followed by a brief stimulation with anti-CD3/CD28 for 3 h and gene expression was assessed by Fluidigm's Biomark high throughput qPCR. We found a marked decrease in *Il9*, *Il17a* and *Ifng* in memory T cells carrying the reference SNP, rs874040^{CC} compared with memory T cells carrying the rs874040^{GG} protective allele (Fig. 3A). Analysis of master regulators of Th1-, Th9- and Th17-cell development, *Stat1*, *Irf4* and *Rorc*, respectively, showed that the presence of the rs874040^{CC} risk allele was associated with lower levels of *Stat1* ($P = 0.02$) while *Irf4* and *Rorc* expression was not significantly changed (Fig. 3B). An expression profile of 84 genes in memory T cells from the three genotyped groups for the rs874040 is shown (Supplementary Material, Table S3). Prior to analysis, we adjusted expression for ethnicity. To account for multiple comparisons, we set the significance threshold to $0.05/84 = 0.000595$. Spearman rank correlations showed a trend of association of *Il9* gene expression and the number of G alleles of rs874040 (0.00076) (Table 3).

Induction of Notch signaling reversed the repressed inflammatory phenotype of rs874040^{CC} memory T cells

Next, we asked whether increased RBPJ levels in rs874040^{CC} memory T cells could alter cytokine production in response to Notch ligation. To address this question, we activated memory CD4$^+$ T cells that were isolated from genotyped healthy subjects of European ancestry with immobilized Notch ligands, DLL4-Fc, Jagged2-Fc or control IgG (2 µg/ml each). Cells were stimulated in serum-free culture T cell-specific X-vivo media in the presence of anti-CD3/CD28 for 7 days, and a panel of cytokines and chemokines was measured with a bead-based Luminex assay using the culture supernatants. Interestingly, we found that memory T cells carrying the rs874040^{CC} risk allele exhibited higher production of the canonical Notch target genes, IL-9 and IL-17A under Jagged2-Fc stimulation. However, DLL4-Fc stimulation

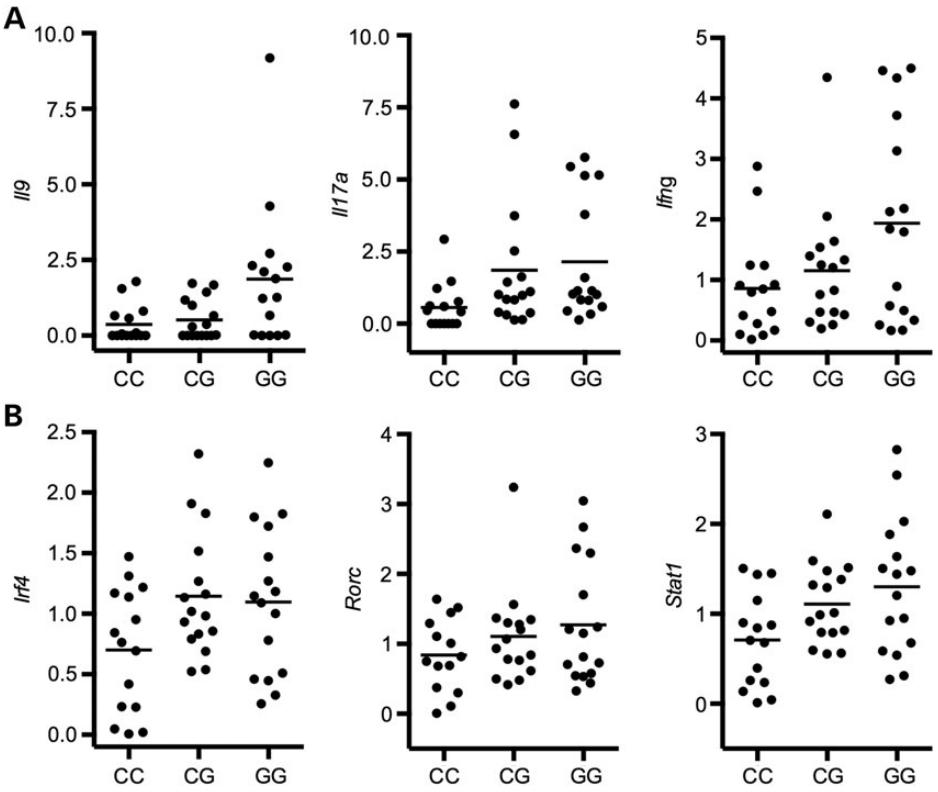

Figure 3. The risk allele rs874040^{C} is associated with repressed inflammatory genes in memory CD4^{+}CD45RO^{+} T cells of healthy genotyped subjects. CD4^{+}CD45RO^{+} memory T cells were isolated from peripheral blood of healthy subjects bearing risk (CC), protective (GG) or heterozygous for the rs874040 allele. Cells were stimulated with anti-CD3/CD28 and the expression of (**A**) *Il9*, *Il17a* and *Ifng* as well as (**B**) *Irf4*, *Rorc* and *Stat1* was measured at the gene level by the Fluidigm BioMark technology. Data are shown at 3 h after stimulation. Groups were compared by one-way ANOVA test. Each dot represents an individual (n = 12–15/group).

Table 3. Spearman rank correlations of gene expression and the number of G alleles of rs874040

Gene	ρ	P-values
IL-9	0.494	0.00076
IFNγ	0.362	0.0159
IL-17A	0.355	0.0179

Bonferroni threshold of 0.05/84 = 0.000595 adjusting for multiple hypothesis.

induces IFNγ and to a lesser extent IL-17A in rs874040^{CC} memory CD4^{+} T cells compared with those bearing the rs874040^{GG} genotype (Fig. 4). We did not detect any significant changes in the production of other effector cytokines including IL-4, IL-5, IL-10, IL-13, IL-21 or IL-22 (data not shown). Spearman rank correlations of cytokine expression and the number of G alleles of rs874040 showed that while DLL4-Fc induces IFNγ expression, Jagged2-Fc induces IL-9 expression below the Bonferroni threshold of 0.05/(20 × 3) = 0.00083 for multiple testing (analysis of 20 cytokines in 3 conditions). A trend of correlation between the number of G alleles of rs874040 and IL-17A expression in Jagged2-Fc-treated cells was observed, but this correlation did not meet the Bonferroni threshold (Table 4).

Memory T cells from RA patients are susceptible to Notch stimulation

Given that the RA rs874040^{CC} risk allele influences the Notch pathway in memory T cells, we sought to analyze Notch signaling in the adaptive immune system of RA patients. Subjects with osteoarthritis, a non-inflammatory musculoskeletal condition were used as controls and were recruited in parallel and screened for the absence of inflammatory diseases. Memory CD4^{+} T cells were isolated from PBMCs of RA and age- and sex-matched control subjects and analysis was carried out in a blinded manner. We first measured *RBPJ* mRNA levels in the RA and control subjects (n = 20/group). Using Taqman qPCR for total *RBPJ*, we found significantly higher expression of RBPJ in memory T cells from RA patients compared with controls (P = 0.02) (Fig. 5A). To analyze the influence of elevated RBPJ expression on memory T-cell phenotypes in RA patients, we measured cytokine secretion in response to Notch signaling activation. Thus, cells from these two groups were activated with anti-CD3/CD28 in the presence of DLL4-Fc, Jagged2-Fc or control IgG for 7 days. Using a Luminex assay, we measured cytokine release of IL-9, IL-17A and IFNγ. Comparing memory T cells from RA patients to their counterparts isolated from control subjects, we found a ligand-specific T-cell differentiation such that Jagged2-Fc skewed the cells from RA patients toward IL-9 and IL-17A production (Fig. 5B and C) whereas DLL4-Fc induced IL-17A and IFNγ (Fig. 5C and D). These findings suggest that Notch signaling may be involved in the enhancement of inflammatory cytokine production in RA patients. To investigate possible disease confounding, we analyzed RBPJ mRNA expression by subdividing the RA patients that are all seropositive for either RF or anti-CCP^{+} into different groups based on disease manifestation and medication. RBPJ expression in RA patients does not segregate with any particular clinical characteristic including disease activity, biological treatment (anti-TNF and Rituximab) or age (Supplementary Material, Fig. S2).

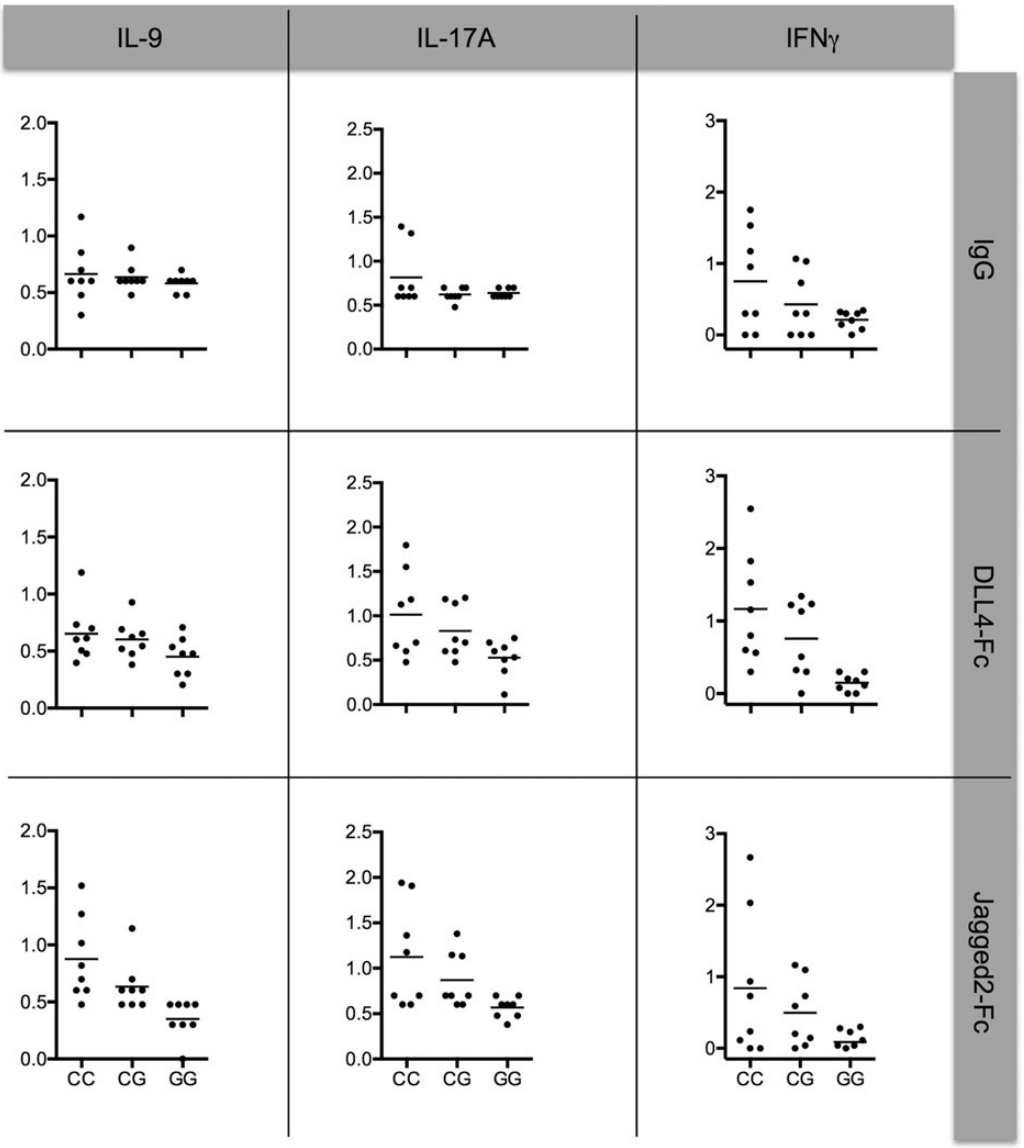

Figure 4. Notch stimulation enhanced inflammatory molecules in the rs874040^{CC} memory T cells of healthy subjects. Memory CD4$^+$CD45RO$^+$ T cells were isolated from peripheral blood of healthy subjects bearing risk (CC), protective (GG) or heterozygous for the rs874040 allele and cells were stimulated for 7 days with anti-CD3/CD28 in the presence of immobilized Delta-like 4 (DLL4-Fc), Jagged2-Fc or control IgG fusion proteins. IL-9, IL-17A and IFNγ production in the culture supernatants was measured by Luminex bead-based assays. Statistical analyses of log10-transformed values were performed by Spearman rank correlations. Each dot represents an individual ($n = 8$/group).

Table 4. Spearman rank correlations of gene expression and the number of G alleles of rs874040

	Gene condition combo	ρ	*P*-values
IFNγ	IFNγ_IgG	−0.258	0.223
	IFNγ_Jagged2-Fc	−0.326	0.121
	IFNγ_DLL4-Fc	−0.714	0.0000904[a]
IL-9	IL9_IgG	−0.157	0.463
	IL9_Jagged2-Fc	−0.763	0.0000146[a]
	IL9_DLL4-Fc	−0.373	0.0724
IL-17A	IL17A_IgG	−0.168	0.431
	IL17A_Jagged2-Fc	−0.567	0.00386
	IL17A_DLL4-Fc	−0.433	0.0347

[a]Below Bonferroni threshold of 0.05/60 = 0.00083 adjusting for multiple hypothesis.

Discussion

Many autoimmune diseases, including RA, are driven by self-reactive Th cells. Until recently, organ-specific autoimmune diseases were primarily associated with Th1 cells. However, the discovery of a number of new effector T-cell subsets, such as Th17, Th9 and regulatory T cells (Treg), such as CD4$^+$FoxP3$^+$ Tregs, have changed the way we view and understand auto-immunity at both the cellular and molecular levels (33). In the present study, we demonstrated that memory CD4$^+$ T cells carrying the RA-associated rs874040 polymorphism in the *RBPJ* gene region, that is in high LD ($r^2 = 0.97$; $D' = 0.99$) with a SNP associated with risk of type 1 diabetes (T1D, rs10517086), exhibit an altered phenotype through the activation of Notch signaling. We found that rs932036 that is in high LD with the reference rs874040 SNP overlaps with the enhancer boundaries upstream of the *RBPJ*

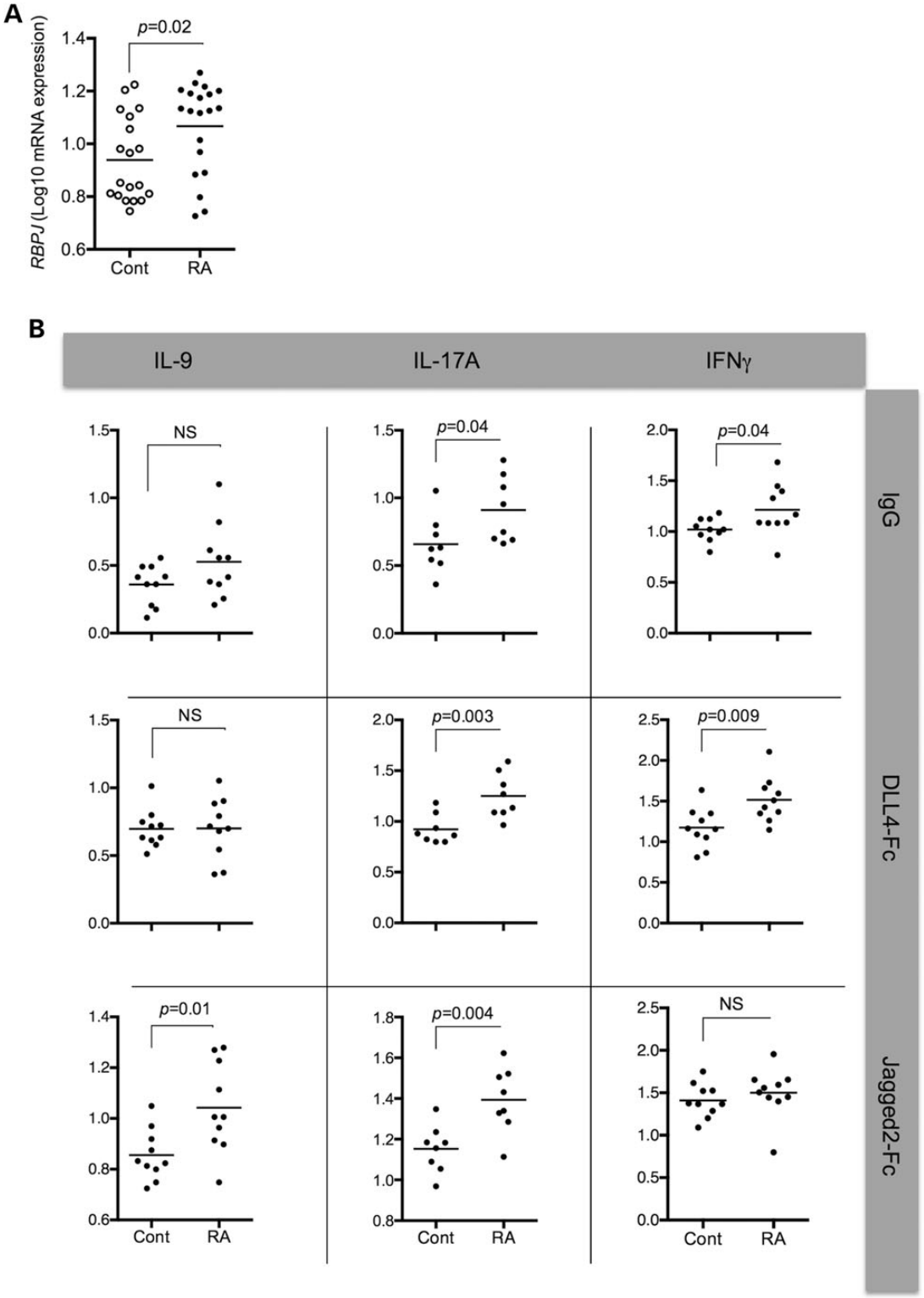

Figure 5. Elevated RBPJ expression and Notch signaling in memory T cells of RA patients. Memory $CD4^{+}CD45RO^{+}$ T cells were isolated from frozen PBMCs of RA patients and control subjects affected with a non-inflammatory musculoskeletal condition. (**A**) RBPJ mRNA was measured by Taqman PCR 3 h following memory T cells stimulation with anti-CD3/CD28 ($n = 20$/group). (**B**) Cells were stimulated for 7 days with anti-CD3/CD28 in the presence of immobilized DLL4-Fc, Jagged2-Fc or control IgG. Culture supernatants were collected and the expression of IL-9, IL-17A and IFNγ was measured by Luminex bead-based assays. Statistical analyses of log10-transformed values were performed by the Student *t*-test. Each dot represents an individual ($n = 8$–10/group).

promoter in memory, but not naive T cells suggesting that rs932036 may be involved in the regulation of the memory T-cell phenotype. Interestingly, memory T cells from healthy individuals bearing the $rs874040^{CC}$ risk variant produced more IL-9/IL-17A or IFNγ in response to Jagged2 and DLL4 ligation, respectively (Fig. 6). We also found that peripheral memory T

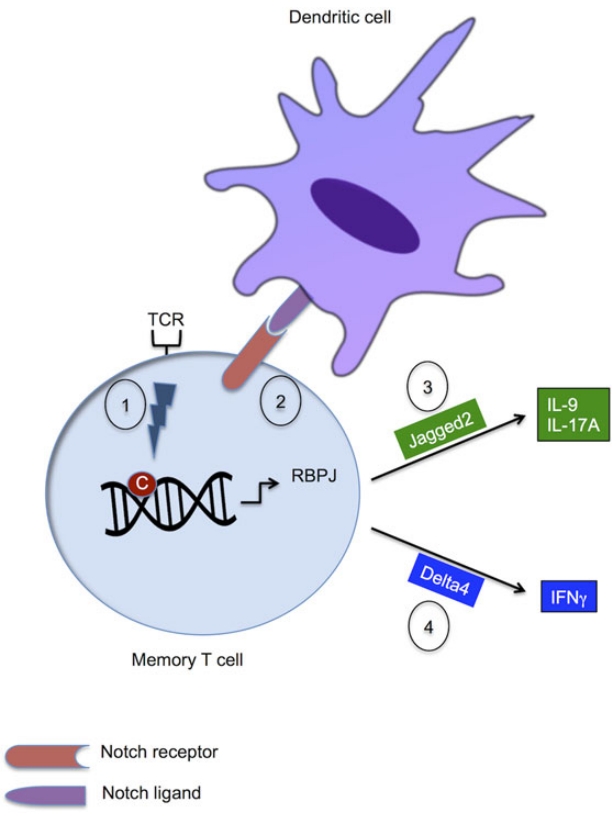

Figure 6. The summary of the involvement of rs874040 and RBPJ in the regulation of memory CD4$^+$ T-cell phenotype. The rs874040 lays over an enhancer region upstream of the TSS of *RBPJ*, a transcriptional repressor that is involved in the differentiation of T cells. We detected a higher expression of *RBPJ* in memory, but not in naive T cells exposed to TCR signaling (1). Induction of canonical Notch signaling in memory CD4$^+$ T cells carrying the reference rs874040 risk allele (2) using two soluble forms of Notch ligands, Jagged2 (3) or DLL4 (4), differentiated memory T cells into IL-9/IL-17A or IFNγ producers, respectively.

cells from RA patients expressed elevated levels of RBPJ, compared with control subjects with a non-inflammatory musculoskeletal condition, leading to the production of inflammatory cytokines upon Notch ligation.

Epigenetics and memory T cells in RA

The etiological paradigm of RA is that an environmental trigger in a genetically predisposed individual can induce autoimmune responses (34). Although genetic factors play a major role, the low concordance rate (~12%) observed in RA between monozygotic twins suggests that epigenetic factors are important in the development and progression of RA. This is supported by chromatin-state annotation studies that have emerged as a powerful approach for discovering regulatory regions and their cell type-specific activity patterns. For instance, it has been shown recently that Treg suppressive function in RA patients is defective and that methotrexate treatment restores Treg function through demethylation of the Foxp3 upstream enhancer in patients with RA (35). Another example of how small epigenetic changes can impact the adaptive immune system is reflected by the methylation of a single CpG site in the promoter of cytotoxic T-lymphocyte-associated protein 4 (CTLA-4) in Tregs of RA patients that resulted in impaired binding of the transcription factor nuclear factor of activated T cells 2 leading to decreased expression levels of CTLA-4 and reduced Treg suppressive function in RA patients compared with healthy controls (36). In our present study, analysis of the chromatin state in naïve and memory T cells revealed the presence of transcriptional enhancers predominantly in the rs874040 LD block in memory T cells. Specifically, we identified rs932036 that is in high LD with the reference SNP rs874040 overlaps with both enhancer boundaries and a potential binding site for the transcription factor ELK1 that is an early response transcription activator and is involved in the induction of the early growth response signaling in T cells (29–31). It should be noted that higher RBPJ expression in memory T cells carrying the rs874040 risk allele was detected following a brief TCR crosslinking (3 h), suggesting the involvement of a transcription factor downstream of TCR signaling. These findings suggest that the rs932036 risk variant may be involved in the differential *RBPJ* transcription in memory versus naïve CD4$^+$ T cells.

Several studies have investigated tissue-specific patterns in RA loci. Tissue-specific expression of RA loci genes and overlap of RA risk SNPs with tissue-specific active regulatory elements showed that the RA risk loci are enriched for genes specifically expressed in CD4$^+$ T cells, CD4$^+$ memory T cells and regulatory T cells (37). It is intriguing that auto-reactive T cells in RA patients that are found in the synovial joint tissue are predominantly memory CD4$^+$ cells (38). Memory CD4$^+$ T cells have several advantages over their naïve and effector counterparts particularly their survival advantage (39). It is intriguing that a recent report showed that RBPJ is required for murine memory CD4$^+$ T-cell survival (40). This finding is in agreement with our observation revealing higher counts of recovered memory T cells from healthy subjects bearing the rs874040 risk allele (data not shown). These data suggest that elevated RBPJ levels associated with the RA risk may contribute to enhanced pathogenic memory T cells in RA patients.

Role of Notch pathway in autoimmunity, ligand expression in RA synovium

Notch receptors and ligands are expressed on both innate and adaptive immune cells and their expression is inducible in response to specific inflammatory signals. Notch receptors are expressed on naïve CD4$^+$ T cells but they are up-regulated on memory CD4$^+$ T cells (40). Dendritic cells displayed distinct expression profiles of Delta and Jagged when exposed to biologically relevant pathogen preparations associated with a specific Th phenotype. For instance, expression of DLL4 was increased, while Jagged2 decreased in dendritic cells stimulated with Th1-promoting bacterium *Propionibacterium acnes* (41). It should be mentioned that *P. acnes* has been isolated from involved joints in rare cases of RA and chronic juvenile arthritis, presumably as a result of bacterial inoculation, usually during infiltration (42). Other reports showed that expression of DLL4 is elevated on dendritic cells after respiratory syncytial virus (43). In our study, we show that Jagged2 and DLL4 promote distinct memory T-cell phenotypes associated with the rs874040 risk allele as Jagged2 induces IL-9/IL-17A expression while DLL4 promotes IFNγ production. The functional involvement of Notch signaling in the pathophysiology of RA has been demonstrated previously using cultured synoviocytes. It has been shown that the expression of Notch 1, Notch 4 and Jagged2 are up-regulated in the RA synovium based on a comparative study of cultured synoviocytes treated with TNFα (44). Nakazawa *et al.* also demonstrated that inhibition of endogenous Notch 1 expression led to the suppression of TNFα-induced synovial proliferation. In addition, a γ-secretase inhibitor that blocks proteolysis of adjacent membrane

portions, also suppressed TNFα-induced synovial proliferation (45). Although the functional difference between Notch 1 to Notch 4 remains obscure, these results indicate that Notch signaling plays a variety of roles in the pathophysiology of RA.

Role of cytokines in RA

Cytokines are attractive therapeutic targets in autoimmune arthritis. Despite the broad spectrum of anti-rheumatic drugs including anti-TNF inhibitors, RA is still not well controlled in up to 30% of patients (46). Th17 cells have been implicated in the pathogenesis of most common autoimmune diseases, including RA, psoriasis, inflammatory bowel disease and multiple sclerosis. Although anti-IL-17A antibodies show marked clinical efficacy in psoriasis, targeting IL-17A alone is not sufficient to improve clinical end-points in other autoimmune conditions, namely RA. Given that Th17 cells express IL-17A together with many other inflammatory cytokines (IL-9, IL-17F, IL-22 and IFNγ) (47–49) and IFNγ (50–52), targeting the Th17-cell lineage may be superior to blocking a single effector cytokine. In our present study, we showed that the CC genotype at the *RBPJ* risk locus increases the susceptibility of memory T cells to co-produce IL-9/IL-17A or IFNγ upon stimulation with Jagged2 or DLL4, respectively.

The involvement of IL-17A in autoimmune arthritis is well documented. IL-17A induces migration of neutrophils to inflammatory joints and acts on a broad range of cell types to produce inflammatory cytokines, including IL-1β, TNFα and IL-6 (53). IL-17A also helps B cells to produce antibodies (54) and IL-17A deletion ameliorates disease symptoms in a mouse model of autoimmune arthritis (55). In addition, a polymorphism in *CCR6*, which is predominantly expressed in human Th17 cells, is associated with RA susceptibility (7).

To date, no direct link between IL-9 and autoimmune arthritis has been demonstrated, although a number of studies pointed to a possible involvement of IL-9 in disease regulation. First, Khan *et al.* (56) reported that in the plasma of RA patients who received rituximab therapy, an anti-CD20 depleting antibody, IL-9 was elevated in patients who responded to therapy. Secondly, a genetic study identified polymorphisms in the *IL-9R* loci that have been linked to genetic susceptibility of RA and allergic diseases (57). Thirdly, in a prospective cohort of first-degree relatives of RA probands, a population without RA but at increased risk for its future development, IL-6 and IL-9 were associated with both rheumatoid factor and a high-risk autoantibody profile (58). IL-9 is a pleiotropic cytokine that exerts autocrine and paracrine activities thus playing a critical role in the development and regulation of autoimmune and allergic diseases (47,59). The IL-9 receptor (IL-9R) is expressed on many hematopoietic cells including T (60,61) and B cells (62). In human $CD4^+$ Th cells, blocking IL-9 with neutralizing antibody strongly inhibited subsequent upregulation of IL-9, IFNγ and IL-17 in skin Th cells (63). In line with these findings, our group and others have demonstrated that anti-IL-9 suppresses Th17-cell development in the animal model of multiple sclerosis (21,48,64). Another study showed that the addition of recombinant IL-9 to memory B cells potentiates IL-4-mediated antibody production (62), a promising cell target for RA (65). These reports suggest that IL-9 exerts autocrine and paracrine activities and that rs874040 risk-mediated increased IL-9 production may contribute to the disease activation by enhancing T- and B-cell activation inflammatory responses.

IFNγ had been originally identified as a Th1 cytokine but recent reports in mice and humans showed that IFNγ is a key component of pathogenic Th17 cells and is required for the pathogenicity of these cells as revealed by increasing recognition of IL-17/IFNγ double-positive Th cells in several human autoimmune diseases including arthritis (66). Recent studies showed that Th1 cells are more frequently observed than Th17 cells and self-antigen-specific Th1 cells are detected in RA synovial fluid. As for the function, Th1-derived IFNγ may play a role in inflammatory responses. However, Th1 cells exert anti-osteoclastogenic effects via IFNγ and IFNγ receptor-deficient mice exhibit more severe symptoms in autoimmune arthritis (67), suggesting that Th1 cells may not suppress the bone destruction phase in arthritic mice (68). However, the role of Th1 cells in RA pathogenesis is still to be determined.

Small molecule inhibitors targeting the Janus kinase (JAK) pathway are a promising new treatment strategy for RA. JAK signaling regulates numerous cytokines and growth factors. In murine T cells, JAK inhibition suppresses IL-17A production (69). We have recently showed that of JAK3/STAT5 signaling regulates *Il9* promoter transcription and genetic and pharmacological inhibition of JAK/STAT suppresses IL-9 expression (70). Notch maybe a promising therapeutic target in RA. Indeed, Notch signaling was found to be activated in $CD4^+$ T cells and synovial tissue from collagen-induced arthritis mice and administration of the γ-secretase inhibitor, DAPT, that blocks Notch activation substantially reduced the severity of arthritic symptoms and joint damage in collagen-induced arthritis mice via suppression of Th1 and Th17 immune responses (22,71).

Conclusion

The present study implicates an RA-associated polymorphism in the development of a specific inflammatory phenotype of memory T cells under the control of Notch signaling. This finding elucidates a novel target pathway for potential drug development identified through genetic studies followed by deep immunophenotyping.

Materials and Methods

The Brigham & Women's Hospital PhenoGenetic project

Peripheral venous blood was obtained from healthy control volunteers in compliance with protocols approved by the Institutional Review Board of Partners Healthcare. The PhenoGenetic Project is a living tissue bank that consists of healthy subjects that are re-contactable based on their genotype. 1741 healthy subjects more than 18 years old have been recruited from the general population of Boston, MA, USA. They are free of chronic inflammatory, infectious and metabolic diseases. Their median age is 24, and 62.7% of subjects are women. Subjects from the Brigham & Women's Hospital (BWH) PhenoGenetic Project were genotyped using DNA isolated from whole blood and the iPLEX™ Sequenom MassARRAY platform (genotype call rate > 95%, Hardy–Weinberg equilibrium $P > 0.001$).

Genotyping and imputation

Each subject was genotyped using the Illumina Infinium Human OmniExpress Exome BeadChips, which includes genome-wide genotype data as well as genotypes for rare variants from 12 000 exomes as well as common coding variants from the whole genome. The LD scores were calculated using data from the CEU (population originating from Northwestern Europe) population of the 1000 Genomes Project. The recombination rate was estimated from HapMap samples. In total, 951 117 SNPs were genotyped, of which 704 808 SNPs are common

variants [minor allele frequency (72) >0.01] and 246 229 SNPs are exomic variants. The genotype success rate was ≥97%. We applied rigorous subject and SNP quality control that includes (i) gender misidentification (ii) subject relatedness (iii) Hardy–Weinberg equilibrium testing (iv) use concordance to infer SNP quality (v) genotype call-rate (vi) heterozygosity outlier (vii) subject mismatches. In the European population, we excluded 1987 SNPs with a call rate of <95%, 459 SNPs with Hardy–Weinberg equilibrium $P < 10^{-6}$, and 63 781 SNPs with MAF < 1% from the 704 808 common SNPs (a total of 66 461 SNPs excluded).

RA studies

RA patients were recruited from the Brigham and Women's Hospital Arthritis Center. All RA patients met the 2010 American College of Rheumatology—European League Against Rheumatism classification criteria for RA and had either a positive rheumatoid factor or anti-cyclic citrullinated peptide antibody test. Disease activity varied from high disease activity to remission, and the average serum C-reactive protein level was 8.3 mg/l (range, 0.3–50.8). DMARD therapy in this cohort included methotrexate (1), anti-TNF therapy (7), rituximab (4), tocilizumab (2), azathioprine (1), sulfasalazine (1), hydroxychloroquine (3) or none (4). Control patients presenting to the Arthritis Center for treatment of a non-inflammatory musculoskeletal condition were recruited in parallel and screened for the absence of inflammatory diseases before inclusion.

Memory cell isolation and treatment

PBMCs were separated by Ficoll-Paque PLUS (GE Healthcare, Piscataway, NJ, USA) gradient centrifugation. PBMCs were frozen at a concentration of 1–3 × 10^7 cells/ml in 10% DMSO (Sigma-Aldrich, St Louis, MO, USA)/90% FBS (Atlanta Biologicals, Lawrenceville, GA, USA). After thawing, PBMCs were washed in 10 ml PBS (Lonza). Untouched T-cell populations were isolated by negative selection using magnetic bead separation of human naïve $CD4^+$ $CD45RO^-CD45RA^+$ and memory $CD4^+CD45RA^-CD45RO^+$ T cells (Miltenyi Biotech, Inc., Auburn, CA, USA) with MACS LS Columns on a MACS Separator magnet (Miltenyi Biotech, Inc.). Isolated cells were quantified on a Nexcelom Bioscience Cellometer® cell counter using Cellometer ViaStain AOPI dual-fluorescence dye. T cells were plated equally at 20 000–50 000 cells per well on 96-well round bottom polystyrene culture plates (Costar). Recombinant human Jagged2-Fc, DLL4-Fc and control IgG were purchased from R&D Systems. Naïve and memory $CD4^+$ T cells were incubated at 37°C (5% CO_2) for 0 h, 3 h or 7 days in RPMI 1640 Medium (Gibco) with plate-bound Jagged2-Fc, DLL4-Fc or IgG (2 µg/ml) in the presence of immobilized anti-CD3 [OKT3 (trade name Orthoclone)]/soluble CD28 (1 µg/ml) (Biolegend) and soluble IL-2 (20 U/ml).

High throughput qPCR (Fluidigm Biomark)

A comprehensive analysis of gene expression in memory $CD4^+$ T cells was performed using Fluidigm's Biomark high throughput qPCR chip. This system utilizes microfluidic technology to perform high throughput gene expression measurements with real-time PCR. We examined the expression of 84 genes in T cells from 46 healthy individuals. These genes were selected based on previously described function of Notch signaling in T cells. Additional genes involved in T-cell function were included in the panel as an exploratory mechanism. Memory T cells were plated at a density of 1×10^5 cells per well in a 96-well plate and were activated with anti-CD3/CD28 for 3 h. RNA was extracted from each sample using an Absolutely RNA 96 Microprep Kit (Agilent) and equalized to 1 ng/ul followed by conversion to cDNA. Individual samples and gene expression assays were pipetted into the microfluidic chip and mixed. Thermal cycling was performed, the chip was imaged at the end of each cycle and analysis software generated PCR curves for each of the wells. Data were analyzed using the ΔΔCT method and expression was normalized to GAPDH.

Luminex assay

For the measurement of cytokines in cultures, cells were grown in serum-free X-vivo media and supernatants were collected on Day 7 after Notch ligation and the secreted cytokines were determined by the fluorescent bead-based Luminex technology (Luminex, Austin, TX, USA) for the indicated cytokines, in accordance with the manufacturers' instructions. These cytokines are: GM-CSF, IFNγ, IL-1b, IL-4, IL-5, IL-6, IL-9, IL-10, IL-13, IL-12p70, IL-15, IL-17A, IL-17F, IL-22, IL-23, IL-27, IL-28A, IL-31, IL-33 and CCL20.

RNA interference

To knockdown the expression of *RBPJ*, $CD4^+$ T cells were purified using MACS beads and nucleoporated with small interfering RNA (siRNA) specific for human *RBPJ* (Santa Cruz Biotechnology). Scrambled siRNA was used as control. Cells were transfected using an Amaxa nucleoporator system. Briefly, $5–10 \times 10^6$ $CD4^+$ T cells were resuspended in 100 µl Nucleofector solution and transfected with 100 nM siRNA using Amaxa Nucleofector (Lonza, Basel, Switzerland). After transfection, the cells were incubated for 4 h at 37°C, medium was changed followed by activation with anti-CD3/CD28 (1 µg/ml each) for 24 h. The efficiency of the knockdown was verified by Taqman PCR. For this, RNA was purified using Stratagene RNA kit and transferred directly into the RT reagent using the Applied Biosystems Taqman reverse transcriptase reagents. Samples were subjected to real-time PCR analysis on PRISM 7000 Sequencer Detection System (Applied Biosystems, Foster City, CA, USA) under standard conditions. Genes analyzed were detected using commercially available assays (Applied Biosystems). Relative mRNA abundance was normalized against GAPDH.

Taqman PCR

RNA was isolated using the Stratagene kit (Agilent Technologies, Palo Alto, CA, USA) and converted to cDNA via reverse transcriptase by random hexamers and Multiscribe RT (TaqMan Gold RT-PCR kit, Applied Biosystems, Foster City, CA, USA). The primers used for this study were purchased from Applied Biosystems. The values are represented as the difference in *Ct* values normalized to β2-microglobulin for each sample as per the following formula: relative RNA expression = $(2^{-dCt}) \times 10^3$.

Statistical analysis

Statistical analysis was performed using Prism, version 5.0 and R version 3.2.1. Results in Table 1 were produced using Spearman rank correlations with G as the reference allele. *P*-values in Figure 2B and C were produced by applying one-way analysis of variance (ANOVA). Data in Figures 2D and E were analyzed using unpaired *t*-tests. Prior to analysis of the Fluidigm cytokine expression data in Figure 3, we created residual cytokine expression adjusting for ethnicity with linear regression in the subjects of European ($n = 34$) and African descent ($n = 10$). These residuals

were then analyzed using Spearman rank correlations with G as the reference allele. In Figure 3, where we examine the three primary cytokines of interest, we used a Bonferroni threshold of 0.05/3 = 0.0167 to determine a statistical significance adjusting for multiple testing. Spearman correlations were also used to analyze data in Figure 4, where we applied a Bonferroni threshold of 0.05/9 = 0.0056 to determine the significance adjusting for multiple testing. All subjects plotted in Figure 4 were of European descent. Results in Figure 5 were produced using unpaired *t*-tests.

Supplementary Material

Supplementary Material is available at *HMG* online.

Authors' Contributions

W.E. and E.M.B. conceived and designed the study. W.O., A.R.M., R.B. and M.F. performed wet lab experiments. C.W. performed statistical analysis. H.-U.K., G.S., J.R. and T.R. carried out computational analysis. M.C. and N.C. recruited and processed the PhenoGenetic blood samples. W.O. and W.E. compiled the data and conducted the analysis. S.J.K. and E.W.K. provided critical comments. P.D.J. provided the PhenoGenetic blood samples and critical comments. M.B.B. and D.R. provided RA and control blood samples and clinical data. W.O., W.E. and E.M.B. wrote the manuscript.

Acknowledgements

The authors are grateful to the participants in the Brigham & Women's PhenoGenetic study. We also thank RA patients for their generous blood donations.

Conflict of Interest statement. None declared.

Funding

The research was supported by Awards from the Massachusetts Life Sciences Center and the Biomedical Research Institute at the Brigham and Women's Hospital (RG110219 to W.E.), the American Diabetes Association and the Boston Area Diabetes Endocrinology Research Center (BADERC) (7-12-JF-09 and P30DK057521 to E.M.B.).

References

1. Begovich, A.B., Carlton, V.E., Honigberg, L.A., Schrodi, S.J., Chokkalingam, A.P., Alexander, H.C., Ardlie, K.G., Huang, Q., Smith, A.M., Spoerke, J.M. *et al.* (2004) A missense single-nucleotide polymorphism in a gene encoding a protein tyrosine phosphatase (PTPN22) is associated with rheumatoid arthritis. *Am. J. Hum. Genet.*, **75**, 330–337.
2. Plenge, R.M., Padyukov, L., Remmers, E.F., Purcell, S., Lee, A.T., Karlson, E.W., Wolfe, F., Kastner, D.L., Alfredsson, L., Altshuler, D. *et al.* (2005) Replication of putative candidate-gene associations with rheumatoid arthritis in >4000 samples from North America and Sweden: association of susceptibility with PTPN22, CTLA4, and PADI4. *Am. J. Hum. Genet.*, **77**, 1044–1060.
3. Thomson, W., Barton, A., Ke, X., Eyre, S., Hinks, A., Bowes, J., Donn, R., Symmons, D., Hider, S., Bruce, I.N. *et al.* (2007) Rheumatoid arthritis association at 6q23. *Nat. Genet.*, **39**, 1431–1433.
4. Plenge, R.M., Seielstad, M., Padyukov, L., Lee, A.T., Remmers, E.F., Ding, B., Liew, A., Khalili, H., Chandrasekaran, A., Davies, L.R. *et al.* (2007) TRAF1-C5 as a risk locus for rheumatoid arthritis—a genomewide study. *N. Engl. J. Med.*, **357**, 1199–1209.
5. Gregersen, P.K., Amos, C.I., Lee, A.T., Lu, Y., Remmers, E.F., Kastner, D.L., Seldin, M.F., Criswell, L.A., Plenge, R.M., Holers, V.M. *et al.* (2009) REL, encoding a member of the NF-kappaB family of transcription factors, is a newly defined risk locus for rheumatoid arthritis. *Nat. Genet.*, **41**, 820–823.
6. Raychaudhuri, S., Remmers, E.F., Lee, A.T., Hackett, R., Guiducci, C., Burtt, N.P., Gianniny, L., Korman, B.D., Padyukov, L., Kurreeman, F.A. *et al.* (2008) Common variants at CD40 and other loci confer risk of rheumatoid arthritis. *Nat. Genet.*, **40**, 1216–1223.
7. Stahl, E.A., Raychaudhuri, S., Remmers, E.F., Xie, G., Eyre, S., Thomson, B.P., Li, Y., Kurreeman, F.A., Zhernakova, A., Hinks, A. *et al.* (2010) Genome-wide association study meta-analysis identifies seven new rheumatoid arthritis risk loci. *Nat. Genet.*, **42**, 508–514.
8. Okada, Y., Wu, D., Trynka, G., Raj, T., Terao, C., Ikari, K., Kochi, Y., Ohmura, K., Suzuki, A., Yoshida, S. *et al.* (2014) Genetics of rheumatoid arthritis contributes to biology and drug discovery. *Nature*, **506**, 376–381.
9. Firestein, G.S. (2003) Evolving concepts of rheumatoid arthritis. *Nature*, **423**, 356–361.
10. Nanki, T., Hayashida, K., El-Gabalawy, H.S., Suson, S., Shi, K., Girschick, H.J., Yavuz, S. and Lipsky, P.E. (2000) Stromal cell-derived factor-1-CXC chemokine receptor 4 interactions play a central role in CD4+ T cell accumulation in rheumatoid arthritis synovium. *J. Immunol.*, **165**, 6590–6598.
11. Nanki, T. and Lipsky, P.E. (2000) Cytokine, activation marker, and chemokine receptor expression by individual CD4(+) memory T cells in rheumatoid arthritis synovium. *Arthritis Res.*, **2**, 415–423.
12. Fan, L., Wang, Q., Liu, R., Zong, M., He, D., Zhang, H., Ding, Y. and Ma, J. (2012) Citrullinated fibronectin inhibits apoptosis and promotes the secretion of pro-inflammatory cytokines in fibroblast-like synoviocytes in rheumatoid arthritis. *Arthritis Res. Ther.*, **14**, R266.
13. Bassil, R., Orent, W. and Elyaman, W. (2013) Notch signaling and T-helper cells in EAE/MS. *Clin. Dev. Immunol.*, **2013**, 570731.
14. Amsen, D., Antov, A. and Flavell, R.A. (2009) The different faces of Notch in T-helper-cell differentiation. *Nat. Rev. Immunol.*, **9**, 116–124.
15. Bassil, R., Zhu, B., Lahoud, Y., Riella, L.V., Yagita, H., Elyaman, W. and Khoury, S.J. (2011) Notch ligand delta-like 4 blockade alleviates experimental autoimmune encephalomyelitis by promoting regulatory T cell development. *J. Immunol.*, **187**, 2322–2328.
16. Kared, H., Adle-Biassette, H., Fois, E., Masson, A., Bach, J.F., Chatenoud, L., Schneider, E. and Zavala, F. (2006) Jagged2-expressing hematopoietic progenitors promote regulatory T cell expansion in the periphery through notch signaling. *Immunity*, **25**, 823–834.
17. Amsen, D., Antov, A., Jankovic, D., Sher, A., Radtke, F., Souabni, A., Busslinger, M., McCright, B., Gridley, T. and Flavell, R.A. (2007) Direct regulation of Gata3 expression determines the T helper differentiation potential of Notch. *Immunity*, **27**, 89–99.
18. Fang, T.C., Yashiro-Ohtani, Y., Del Bianco, C., Knoblock, D.M., Blacklow, S.C. and Pear, W.S. (2007) Notch directly regulates Gata3 expression during T helper 2 cell differentiation. *Immunity*, **27**, 100–110.
19. Minter, L.M., Turley, D.M., Das, P., Shin, H.M., Joshi, I., Lawlor, R.G., Cho, O.H., Palaga, T., Gottipati, S., Telfer, J.C. *et al.* (2005)

Inhibitors of gamma-secretase block in vivo and in vitro T helper type 1 polarization by preventing Notch upregulation of Tbx21. *Nat. Immunol.*, **6**, 680–688.
20. Keerthivasan, S., Suleiman, R., Lawlor, R., Roderick, J., Bates, T., Minter, L., Anguita, J., Juncadella, I., Nickoloff, B.J., Le Poole, I.C. *et al.* (2011) Notch signaling regulates mouse and human Th17 differentiation. *J. Immunol.*, **187**, 692–701.
21. Elyaman, W., Bassil, R., Bradshaw, E.M., Orent, W., Lahoud, Y., Zhu, B., Radtke, F., Yagita, H. and Khoury, S.J. (2012) Notch receptors and Smad3 signaling cooperate in the induction of interleukin-9-producing T cells. *Immunity*, **36**, 623–634.
22. Jiao, Z., Wang, W., Hua, S., Liu, M., Wang, H., Wang, X., Chen, Y., Xu, H. and Lu, L. (2014) Blockade of Notch signaling ameliorates murine collagen-induced arthritis via suppressing Th1 and Th17 cell responses. *Am. J. Pathol.*, **184**, 1085–1093.
23. Yavartanoo, M. and Choi, J.K. (2013) ENCODE: a sourcebook of epigenomes and chromatin language. *Genomics Inform.*, **11**, 2–6.
24. Johnson, A.D., Handsaker, R.E., Pulit, S.L., Nizzari, M.M., O'Donnell, C.J. and de Bakker, P.I. (2008) SNAP: a web-based tool for identification and annotation of proxy SNPs using HapMap. *Bioinformatics*, **24**, 2938–2939.
25. Ramos, P.S., Criswell, L.A., Moser, K.L., Comeau, M.E., Williams, A.H., Pajewski, N.M., Chung, S.A., Graham, R.R., Zidovetzki, R., Kelly, J.A. *et al.* (2011) A comprehensive analysis of shared loci between systemic lupus erythematosus (SLE) and sixteen autoimmune diseases reveals limited genetic overlap. *PLoS Genet.*, **7**, e1002406.
26. Ernst, J. and Kellis, M. (2012) ChromHMM: automating chromatin-state discovery and characterization. *Nat. Methods*, **9**, 215–216.
27. Roadmap Epigenomics, C., Kundaje, A., Meuleman, W., Ernst, J., Bilenky, M., Yen, A., Heravi-Moussavi, A., Kheradpour, P., Zhang, Z., Wang, J. *et al.* (2015) Integrative analysis of 111 reference human epigenomes. *Nature*, **518**, 317–330.
28. Pfizer. (2006–2013) Long-term effectiveness and safety of CP-690,550 for the treatment of rheumatoid arthritis. *ClinicalTrials.gov Identifier: NCT00413699*, https://www.clinicaltrials.gov/ct2/show/results/NCT00413699.
29. Li, W., Whaley, C.D., Bonnevier, J.L., Mondino, A., Martin, M.E., Aagaard-Tillery, K.M. and Mueller, D.L. (2001) CD28 signaling augments Elk-1-dependent transcription at the c-fos gene during antigen stimulation. *J. Immunol.*, **167**, 827–835.
30. Xi, H. and Kersh, G.J. (2003) Induction of the early growth response gene 1 promoter by TCR agonists and partial agonists: ligand potency is related to sustained phosphorylation of extracellular signal-related kinase substrates. *J. Immunol.*, **170**, 315–324.
31. Cianferoni, A., Massaad, M., Feske, S., de la Fuente, M.A., Gallego, L., Ramesh, N. and Geha, R.S. (2005) Defective nuclear translocation of nuclear factor of activated T cells and extracellular signal-regulated kinase underlies deficient IL-2 gene expression in Wiskott-Aldrich syndrome. *J. Allergy Clin. Immunol.*, **116**, 1364–1371.
32. Jezierski, A., Ly, D., Smith, B., Smith, C., Tremblay, R., Gruslin, A., Sikorska, M. and Bani-Yaghoub, M. (2010) Novel RBPJ transcripts identified in human amniotic fluid cells. *Stem Cell Rev.*, **6**, 677–684.
33. Jager, A. and Kuchroo, V.K. (2010) Effector and regulatory T-cell subsets in autoimmunity and tissue inflammation. *Scand. J. Immunol.*, **72**, 173–184.
34. Klein, K. and Gay, S. (2015) Epigenetics in rheumatoid arthritis. *Curr. Opin. Rheumatol.*, **27**, 76–82.
35. Cribbs, A.P., Kennedy, A., Penn, H., Amjadi, P., Green, P., Read, J.E., Brennan, F., Gregory, B. and Williams, R.O. (2015) Methotrexate restores regulatory T cell function through demethylation of the foxp3 upstream enhancer in patients with rheumatoid arthritis. *Arthritis Rheumatol.*, **67**, 1182–1192.
36. Cribbs, A.P., Kennedy, A., Penn, H., Read, J.E., Amjadi, P., Green, P., Syed, K., Manka, S.W., Brennan, F.M., Gregory, B. *et al.* (2014) Treg cell function in rheumatoid arthritis is compromised by CTLA-4 promoter methylation resulting in a failure to activate the indoleamine 2,3-dioxygenase pathway. *Arthritis Rheumatol.*, **66**, 2344–2354.
37. Hu, X., Kim, H., Stahl, E., Plenge, R., Daly, M. and Raychaudhuri, S. (2011) Integrating autoimmune risk loci with gene-expression data identifies specific pathogenic immune cell subsets. *Am. J. Hum. Genet.*, **89**, 496–506.
38. Pitzalis, C., Kingsley, G., Murphy, J. and Panayi, G. (1987) Abnormal distribution of the helper-inducer and suppressor-inducer T-lymphocyte subsets in the rheumatoid joint. *Clin. Immunol. Immunopathol.*, **45**, 252–258.
39. Elyaman, W., Kivisakk, P., Reddy, J., Chitnis, T., Raddassi, K., Imitola, J., Bradshaw, E., Kuchroo, V.K., Yagita, H., Sayegh, M.H. *et al.* (2008) Distinct functions of autoreactive memory and effector CD4+ T cells in experimental autoimmune encephalomyelitis. *Am. J. Pathol.*, **173**, 411–422.
40. Maekawa, Y., Ishifune, C., Tsukumo, S., Hozumi, K., Yagita, H. and Yasutomo, K. (2015) Notch controls the survival of memory CD4+ T cells by regulating glucose uptake. *Nat. Med.*, **21**, 55–61.
41. Worsley, A.G., LeibundGut-Landmann, S., Slack, E., Phng, L.K., Gerhardt, H., Reis e Sousa, C. and MacDonald, A.S. (2008) Dendritic cell expression of the Notch ligand jagged2 is not essential for Th2 response induction in vivo. *Eur. J. Immunol.*, **38**, 1043–1049.
42. Kooijmans-Coutinho, M.F., Markusse, H.M. and Dijkmans, B.A. (1989) Infectious arthritis caused by *Propionibacterium acnes*: a report of two cases. *Ann. Rheum. Dis.*, **48**, 851–852.
43. Schaller, M.A., Neupane, R., Rudd, B.D., Kunkel, S.L., Kallal, L.E., Lincoln, P., Lowe, J.B., Man, Y. and Lukacs, N.W. (2007) Notch ligand Delta-like 4 regulates disease pathogenesis during respiratory viral infections by modulating Th2 cytokines. *J. Exp. Med.*, **204**, 2925–2934.
44. Ando, K., Kanazawa, S., Tetsuka, T., Ohta, S., Jiang, X., Tada, T., Kobayashi, M., Matsui, N. and Okamoto, T. (2003) Induction of Notch signaling by tumor necrosis factor in rheumatoid synovial fibroblasts. *Oncogene*, **22**, 7796–7803.
45. Nakazawa, M., Ishii, H., Aono, H., Takai, M., Honda, T., Aratani, S., Fukamizu, A., Nakamura, H., Yoshino, S., Kobata, T. *et al.* (2001) Role of Notch-1 intracellular domain in activation of rheumatoid synoviocytes. *Arthritis Rheum.*, **44**, 1545–1554.
46. O'Dell, J.R., Mikuls, T.R., Taylor, T.H., Ahluwalia, V., Brophy, M., Warren, S.R., Lew, R.A., Cannella, A.C., Kunkel, G., Phibbs, C.S. *et al.* (2013) Therapies for active rheumatoid arthritis after methotrexate failure. *N. Engl. J. Med.*, **369**, 307–318.
47. Elyaman, W., Bradshaw, E.M., Uyttenhove, C., Dardalhon, V., Awasthi, A., Imitola, J., Bettelli, E., Oukka, M., van Snick, J., Renauld, J.C. *et al.* (2009) IL-9 induces differentiation of TH17 cells and enhances function of FoxP3+ natural regulatory T cells. *Proc. Natl Acad. Sci. USA*, **106**, 12885–12890.
48. Nowak, E.C., Weaver, C.T., Turner, H., Begum-Haque, S., Becher, B., Schreiner, B., Coyle, A.J., Kasper, L.H. and Noelle, R.J. (2009) IL-9 as a mediator of Th17-driven inflammatory disease. *J. Exp. Med.*, **206**, 1653–1660.
49. Beriou, G., Bradshaw, E.M., Lozano, E., Costantino, C.M., Hastings, W.D., Orban, T., Elyaman, W., Khoury, S.J., Kuchroo, V.K.,

Baecher-Allan, C. *et al.* (2010) TGF-beta induces IL-9 production from human Th17 cells. *J. Immunol.*, **185**, 46–54.
50. Ghoreschi, K., Laurence, A., Yang, X.P., Tato, C.M., McGeachy, M.J., Konkel, J.E., Ramos, H.L., Wei, L., Davidson, T.S., Bouladoux, N. *et al.* (2010) Generation of pathogenic T(H)17 cells in the absence of TGF-beta signalling. *Nature*, **467**, 967–971.
51. Lee, Y., Awasthi, A., Yosef, N., Quintana, F.J., Xiao, S., Peters, A., Wu, C., Kleinewietfeld, M., Kunder, S., Hafler, D.A. *et al.* (2012) Induction and molecular signature of pathogenic TH17 cells. *Nat. Immunol.*, **13**, 991–999.
52. Kleinewietfeld, M., Manzel, A., Titze, J., Kvakan, H., Yosef, N., Linker, R.A., Muller, D.N. and Hafler, D.A. (2013) Sodium chloride drives autoimmune disease by the induction of pathogenic TH17 cells. *Nature*, **496**, 518–522.
53. Miossec, P., Korn, T. and Kuchroo, V.K. (2009) Interleukin-17 and type 17 helper T cells. *N. Engl. J. Med.*, **361**, 888–898.
54. Hsu, H.C., Yang, P., Wang, J., Wu, Q., Myers, R., Chen, J., Yi, J., Guentert, T., Tousson, A., Stanus, A.L. *et al.* (2008) Interleukin 17-producing T helper cells and interleukin 17 orchestrate autoreactive germinal center development in autoimmune BXD2 mice. *Nat. Immunol.*, **9**, 166–175.
55. Nakae, S., Nambu, A., Sudo, K. and Iwakura, Y. (2003) Suppression of immune induction of collagen-induced arthritis in IL-17-deficient mice. *J. Immunol.*, **171**, 6173–6177.
56. Khan, I.H., Krishnan, V.V., Ziman, M., Janatpour, K., Wun, T., Luciw, P.A. and Tuscano, J. (2009) A comparison of multiplex suspension array large-panel kits for profiling cytokines and chemokines in rheumatoid arthritis patients. *Cytometry B Clin. Cytom.*, **76**, 159–168.
57. Burkhardt, J., Petit-Teixeira, E., Teixeira, V.H., Kirsten, H., Garnier, S., Ruehle, S., Oeser, C., Wolfram, G., Scholz, M., Migliorini, P. *et al.* (2009) Association of the X-chromosomal genes TIMP1 and IL9R with rheumatoid arthritis. *J. Rheumatol.*, **36**, 2149–2157.
58. Hughes-Austin, J.M., Deane, K.D., Derber, L.A., Kolfenbach, J.R., Zerbe, G.O., Sokolove, J., Lahey, L.J., Weisman, M.H., Buckner, J. H., Mikuls, T.R. *et al.* (2011) Multiple cytokines and chemokines are associated with rheumatoid arthritis-related autoimmunity in first-degree relatives without rheumatoid arthritis: Studies of the Aetiology of Rheumatoid Arthritis (SERA). *Ann. Rheum. Dis.*, in press.
59. Stephens, G.L., Swerdlow, B., Benjamin, E., Coyle, A.J., Humbles, A., Kolbeck, R. and Fung, M. (2011) IL-9 is a Th17-derived cytokine that limits pathogenic activity in organ-specific autoimmune disease. *Eur. J. Immunol.*, **41**, 952–962.
60. Demoulin, J.B. and Renauld, J.C. (1998) Interleukin 9 and its receptor: an overview of structure and function. *Int. Rev. Immunol.*, **16**, 345–364.
61. Knoops, L., Louahed, J. and Renauld, J.C. (2004) IL-9-induced expansion of B-1b cells restores numbers but not function of B-1 lymphocytes in xid mice. *J. Immunol.*, **172**, 6101–6106.
62. Fawaz, L.M., Sharif-Askari, E., Hajoui, O., Soussi-Gounni, A., Hamid, Q. and Mazer, B.D. (2007) Expression of IL-9 receptor alpha chain on human germinal center B cells modulates IgE secretion. *J. Allergy Clin. Immunol.*, **120**, 1208–1215.
63. Schlapbach, C., Gehad, A., Yang, C., Watanabe, R., Guenova, E., Teague, J.E., Campbell, L., Yawalkar, N., Kupper, T.S. and Clark, R.A. (2014) Human TH9 cells are skin-tropic and have autocrine and paracrine proinflammatory capacity. *Sci. Transl. Med.*, **6**, 219ra218. doi: 10.1126/scitranslmed.3007828.
64. Li, H., Nourbakhsh, B., Ciric, B., Zhang, G.X. and Rostami, A. (2010) Neutralization of IL-9 ameliorates experimental autoimmune encephalomyelitis by decreasing the effector T cell population. *J. Immunol.*, **185**, 4095–4100.
65. Tedder, T.F. (2009) CD19: a promising B cell target for rheumatoid arthritis. *Nat. Rev.. Rheumatol.*, **5**, 572–577.
66. Nistala, K., Adams, S., Cambrook, H., Ursu, S., Olivito, B., de Jager, W., Evans, J.G., Cimaz, R., Bajaj-Elliott, M. and Wedderburn, L.R. (2010) Th17 plasticity in human autoimmune arthritis is driven by the inflammatory environment. *Proc. Natl Acad. Sci. USA*, **107**, 14751–14756.
67. Vermeire, K., Heremans, H., Vandeputte, M., Huang, S., Billiau, A. and Matthys, P. (1997) Accelerated collagen-induced arthritis in IFN-gamma receptor-deficient mice. *J. Immunol.*, **158**, 5507–5513.
68. Boissier, M.C., Chiocchia, G., Bessis, N., Hajnal, J., Garotta, G., Nicoletti, F. and Fournier, C. (1995) Biphasic effect of interferon-gamma in murine collagen-induced arthritis. *Eur. J. Immunol.*, **25**, 1184–1190.
69. Works, M.G., Yin, F., Yin, C.C., Yiu, Y., Shew, K., Tran, T.T., Dunlap, N., Lam, J., Mitchell, T., Reader, J. *et al.* (2014) Inhibition of TYK2 and JAK1 ameliorates imiquimod-induced psoriasis-like dermatitis by inhibiting IL-22 and the IL-23/IL-17 axis. *J. Immunol.*, **193**, 3278–3287.
70. Bassil, R., Orent, W., Olah, M., Kurdi, A.T., Frangieh, M., Buttrick, T., Khoury, S.J. and Elyaman, W. (2014) BCL6 controls Th9 cell development by repressing Il9 transcription. *J. Immunol.*, **193**, 198–207.
71. Heo, R., Park, J.S., Jang, H.J., Kim, S.H., Shin, J.M., Suh, Y.D., Jeong, J.H., Jo, D.G. and Park, J.H. (2014) Hyaluronan nanoparticles bearing gamma-secretase inhibitor: in vivo therapeutic effects on rheumatoid arthritis. *J. Control. Release*, **192**, 295–300.
72. Naito, T., Tanaka, H., Naoe, Y. and Taniuchi, I. (2011) Transcriptional control of T-cell development. *Int. Immunol.*, **23**, 661–668.